

Angular distribution of parametric (quasi-Cherenkov) radiation

Yu. N. Adishchev, R. B. Babadzhanyan, S. A. Vorob'ev, B. N. Kalinin, V. V. Mun, S. Pak, G. A. Pleshkov, A. P. Potylitsyn, and S. R. Uglov

Kirov Institute of Nuclear Physics, Tomsk Polytechnical Institute

(Submitted 10 December 1986)

Zh. Eksp. Teor. Fiz. **93**, 1943–1950 (December 1987)

The angular distributions of a new type of monochromatic x-ray emission generated by relativistic electrons in single crystals have been measured for the first time. The measurements were performed on single crystals of diamond at $\theta = 90^\circ$ to the direction of the electron beam of energy $E = 900$ and 500 MeV, and on silicon at $\theta = 90^\circ$ and $E = 900$ MeV. All the results are in good agreement with the predictions of the theory of parametric (quasi-Cherenkov) x-ray emission (PXE). Thus, in diamond, the vertical projection of the PXE reflection splits into two peaks, in contrast to the horizontal projection, which does not. In silicon, both projections of the angular distribution are practically symmetric. The width of the angular distributions of PXE is much greater than γ^{-1} where γ is the electron Lorentz factor.

1. INTRODUCTION

An urgent problem in modern physics and technology is the development of strong sources of hard monochromatic radiation, i.e., sources of photons with high spectral and angular density. The possibilities under discussion include the use of the radiation emitted by electrons in synchrotrons, storage rings, and undulators,¹ and also new effects such as ultraviolet and x-ray Cherenkov emission, emission accompanying the channeling of relativistic electrons in crystals, and a number of other phenomena.²⁻⁴ A recent paper⁵ has reported a new technique for producing quasi-monochromatic x radiation, which relies on interference between beams of transition radiation due to intermediate-energy electrons traversing a stack of thin foils.

It is well known that transition radiation is produced when charged particles cross the separation boundary between the two media with different permittivities.⁶ The radiation emitted by a particle moving in a one-dimensional periodic medium consisting of layers with different permittivity was first considered in Ref. 7. Wavelengths of the order of the interatomic separation in the medium are emitted when a relativistic charged particle crosses the atomic planes in a crystal, which provide the necessary change in permittivity. It is expected that a new type of monochromatic x radiation, referred to^{8,9} as parametric (quasi-Cherenkov) x radiation (PXE), will be generated in this way. PXE generation occurs when the periodic disposition of atoms in a crystal ensures that the Vavilov-Cherenkov condition $n > 1$ (n is the refractive index of the medium) is satisfied even in the x-ray range, provided the frequencies ω_B and the photon momenta lie near the edge of the Brillouin zone. In a simple approximation, PXE can be looked upon as a result of the diffraction of the pseudophotons forming the electromagnetic field of a relativistic charged particle by the crystal. Comparison¹⁰ of the spectral and angular characteristics of PXE with other x-ray sources, shows that PXE can have the highest spectral and angular density. The frequency of the radiation can be tuned continuously by rotating the crystal relative to the direction of the incident electron beam. Because of these predictions, PXE is very attractive as a practical source of x rays, and deserves detailed investigation.

A systematic search for the new type of monochromatic

x-rays from relativistic electrons in crystals was carried on the Tomsk synchrotron. The experiments reported in Refs. 11 and 12 were the first in which a line structure was observed in the x-ray spectra due to 900-MeV electrons in diamond. A later paper¹³ reported pbx measurements on single-crystal silicon at the Khar'kov Physicotechnical Institute. A detailed study of the spectrum observed in diamond at $\theta = 2\theta_B = 90^\circ$ (θ_B is the Bragg angle) to the electron beam was reported in Ref. 14. For all the line spectra that were examined,^{11,12-14} the photon energy corresponding to the peaks was exactly equal to the characteristic energies at the PXE frequencies:

$$\omega_B = \pi cn/d \sin \theta_B, \quad n=1, 2, 3, \dots, \quad (1)$$

where d is the separation between the crystal planes and θ_B is the angle between the momentum of the electron and the crystal plane (Bragg angle).

An important feature of PXE that distinguishes it from other sources of x radiation is the angular distribution of the emitted photons. According to the PXE theory,^{8,9} developed without taking dynamic effects into account, the photon angular distribution is asymmetric at large angles (for example, in the geometry used in Refs. 11, 12, and 14), and is split into two individual peaks. The experiments performed on the Tomsk synchrotron¹⁵ were the first attempt to measure the angular distribution of PXE for electrons with energy $E = 900$ MeV in diamond, and a broadening of the PXE reflection was noted. However, these measurements resulted in only a *qualitative* result.

In this paper, we present experimental results on the angular distribution of PXE in diamond at $\theta = 90^\circ$ to the direction of the electron beam with $E = 900$ and 500 MeV, and in silicon at $\theta = 90^\circ$ with $E = 900$ MeV. The results obtained are interpreted in terms of the PXE theory.^{8,9}

2. METHOD OF MEASUREMENT

The measurements were performed in the internal electron beam of the Tomsk synchrotron. The experimental arrangement is described in Ref. 14. Electrons accelerated in the synchrotron vacuum chamber were deflected onto an internal target in the form of a single crystal of diamond or silicon. The thickness of the diamond wafer was 0.35 mm

and the corresponding figure for silicon was 0.37 mm. The electrons were deflected onto a target for a total of 15 ms at a repetition frequency of 4 Hz. The electron beam had an angular divergence of 10^{-4} rad (at electron energy $E = 900$ MeV), and its energy spread was 0.5%. The angular distribution of parametric x-ray emission was measured at $E = 900$ and 500 MeV. The crystal was oriented relative to the electron beam using a goniometer in angular increments of $\Delta\psi_v \approx 2 \times 10^{-5}$ and $\Delta\psi_h \approx 7 \times 10^{-6}$ rad around the vertical and horizontal axes, respectively.

The emission of γ rays by channeled electrons¹⁶ was used to orient the single crystals. The γ rays were recorded by a detector mounted at 20° to the γ -ray beam in Compton-scattering geometry. The Compton target was aluminum, 0.5 mm thick. The number of accelerated electrons was monitored by an inductive current sensor to within 5%, or by a synchrotron radiation sensor to within 20%. The number of electrons deflected onto the target was measured by measuring the total γ -ray energy using a Wilson photon counter. It was assumed that the radiative electron energy loss in an unoriented single crystal was equal to the energy loss in the amorphous medium. The number of electrons was determined, in our case, to within 20%.

The x-ray spectrometer was a proportional counter (SPRO-16), filled with a mixture of xenon and methane (10%). It was equipped with an entrance window in the form of beryllium foil, 4×16 mm² and 0.15 mm thick. The energy resolution of the spectrometer at the K_α line of copper ($\omega_\gamma = 8.05$ keV) and a count rate of 10^4 s⁻¹ was about 20%, and the detection efficiency was up to 60%. The lower detection threshold of the spectrometer corresponded to photon energy $\omega_{th} \approx 3$ keV, and the working range extended up to 30 keV. Another x-ray spectrometer that was used was a scintillation counter incorporating a single crystal of NaI(Tl), 1 mm thick, and the FEU-35A photomultiplier. The entrance window of the detector had a diameter of 22 mm and was made from a beryllium foil, 0.1 mm thick. The energy resolution of the spectrometer at the 14-keV γ -ray line of ⁵⁷Co was 35%. The energy resolution at the 34-keV line of ¹³⁹Ce was about 25%. The energy equivalent of the spectrometer threshold was $\omega_{th} \approx 12$ keV for a detection efficiency of 98%. The NaI(Tl) spectrometer was used to replace the proportional counter under the same shielding.

In this experiment, the accelerated current of electrons in the synchrotron was preset so that the total count in the spectrometer channel was 200 photons or less per electron pulse, which corresponded to $N_e \leq 5 \times 10^8$ electrons per pulse. Under these conditions, the probability of pulse overlapping can be estimated from the formula¹⁷

$$p = [1 - \exp(-N_0 t_1)],$$

where p is the probability that pulses will superimpose, N_0 is the average detector count rate, and t_1 is the duration of the detector signal. In our case, $t_1 \approx 10^{-6}$ s, $N_0 \approx 15000$ s⁻¹, and overlapping of the detector pulses amounted to less than 3%.

The photon angular distributions were measured by scanning the PXE reflections with the collimated x-ray spectrometer along two mutually perpendicular directions. The experiment was performed on-line to the SM-3 computer. Figure 1 shows the geometry of the experiment in which the electron beam was at an angular θ_B to the (100) planes of

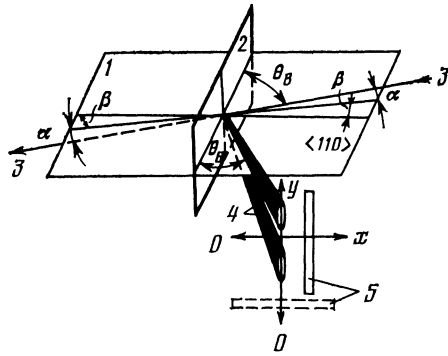


FIG. 1. Geometry of the experiment: 1—the (001) plane of diamond, 2—the (110) plane of diamond, 3—electron beam, 4—(400) reflection, 5—detector with the slit collimator.

diamond. The photons were detected in this case at $\theta = 2\theta_B = 90^\circ$ to the electron beam. The dimensions of the detector collimator slit were 2.5×16 mm, which corresponded to an angular aperture $\Delta\theta_x = \pm 2.5$ mrad and $\Delta\theta_y = \pm 16$ mrad. The computer plus collimator assembly was displaced by step motors along two mutually perpendicular directions (X and Y). The angular distribution was measured by determining the area under the PXE reflection peaks as a function of the position of the detector in space. To determine the area under a peak, the smoothed background spectrum corresponding to the misaligned crystal was fitted to the effect plus background spectrum by means of a normalizing constant, and was then subtracted.¹⁸ The uncertainty in the area under a peak was determined by the statistics with which the spectrum was recorded, and was at most 3–4%. The measured spectra were normalized to the number of transmitted electrons.

3. EXPERIMENTAL RESULTS AND DISCUSSION

Figures 2–4 show the angular distributions for the (400), (220), and (440) x-ray reflections due to electrons with energies $E = 900$ MeV in a diamond single crystal. The corresponding frequencies are, respectively, $\omega_{400} = 9.8$ keV, $\omega_{220} = 6.9$ keV, and $\omega_{440} = 13.9$ keV. The solid curves represent calculations based on PXE theory.⁹ This theory shows that the angular distribution of PXE photons in a given reflection is described by

$$\frac{1}{N_0} \frac{\partial^2 N}{\partial \theta_x \partial \theta_y} = \frac{\theta_x^2 \cos^2 2\theta_B + \theta_y^2}{[\theta_x^2 + \theta_y^2 + \theta_{ph}^2]}, \quad (2)$$

where N_0 is the factor characterizing the absolute PXE yield, $\theta_{x,y} = (\mathbf{k} - \mathbf{k}_B)_{x,y} / \omega_B$ are the projected angles of photon emission $\theta_{ph}^2 = \gamma^{-2} + \theta_s^2 + \omega_p^2 / \omega_B^2$, γ is the electron Lorentz factor, θ_s^2 is the mean square multiple scattering angle in the crystal, and ω_p is the plasma frequency.

The effect of the dimensions of the rectangular entrance window of the detector and of its position relative to the central reflection was taken into account by integrating (2) over the detector aperture with moving integration limits (a and b will denote the linear dimensions of the collimator slit and R the distance between the crystal and the detector). The first integral with respect to θ_x can readily be evaluated analytically and the result is

$$\frac{1}{N_0} \frac{\partial N}{\partial \theta_y} = \frac{1}{2} \frac{\theta_y^2}{(\theta_y^2 + \theta_{ph}^2)} \left(\frac{\theta_x^2}{\theta_x^2 + \theta_y^2 + \theta_{ph}^2} \right)$$

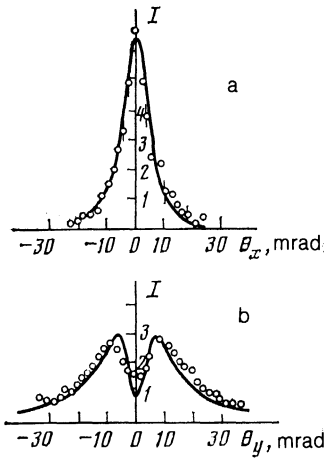


FIG. 2. Angular distribution in the (400) reflection in the horizontal (a) and vertical (b) planes. Solid curves—calculated angular distributions. Electron energy $E = 900$ MeV.

$$+ \frac{\arctan[\theta_x(\theta_y^2 + \theta_{ph}^2)^{-1/2}]}{(\theta_y^2 + \theta_{ph}^2)^{1/2}} \Big|_{\theta_{x1}}^{\theta_{x1} + \alpha/L} \quad (3)$$

The second integral (with respect to θ_y) was evaluated numerically, using (3), between the limits $\theta_{y1} - b/R$, θ_{y1} by the trapezoidal method.

It is clear from Figs. 2–4 that there is reasonable agreement between the measured angular distributions and calculations based on PXE theory.⁹ The total width at half-height of the angular distribution corresponding to the (400) reflection, scanned by the detector along the X direction, is $\Delta\theta_x = 9 \pm 0.5$ mrad, whereas for the (220) reflection the analogous quantity is $\Delta\theta_x = 12 \pm 0.5$ mrad. Finally, for the (440) reflection, we found that $\Delta\theta_x = 7 \pm 0.5$ mrad. It follows that an increase in PXE frequency leads to an appreciable narrowing of its angular distribution for a particular reflection, which is in complete agreement with the theory.⁹ The slit collimator was then placed in a horizontal position, symmetrically relative to the maximum of the distribution along the X axis, and the detector was displaced along the vertical Y axis. It is clear from Figs. 2–4 that, in this case, the angular distribution consists of two separate peaks. The sep-

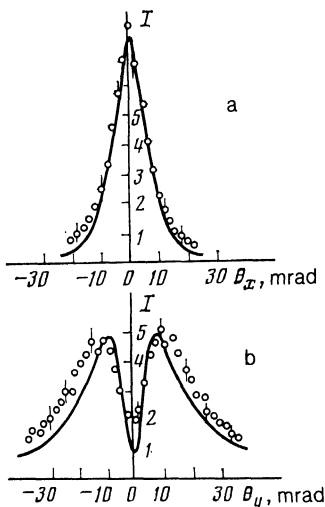


FIG. 3. Angular distribution in the (220) reflection from diamond. The notation is the same as in Fig. 2.

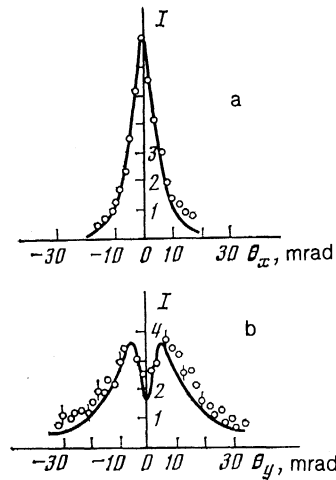


FIG. 4. Angular distribution in the (440) reflection from diamond. The notation is the same as in Fig. 2.

aration between the PXE peaks again decreases with increasing photon frequency, as can be seen by comparing Figs. 3 and 4. The calculated curve is somewhat narrower than the experimental curve, and the depth of the central valley between the peaks is less than the calculated depth. These discrepancies may have been due to inadequate allowance for the angular divergence of the electron beam in the PXE theory,⁸ or to the contribution of real bremsstrahlung photons diffracted by the crystals to the measured angular distribution.

It follows from (2) that a reduction in electron energy should broaden the PXE angular distribution because of the contribution of the γ -factor and the mean square scattering angle $\theta_s^2 = (E_s/E)^2 (L/L_R)$, where $E_s = 21$ MeV and L_R is the radiation length. Figure 5 shows the angular distributions for the (220) and (400) reflections, recorded, respectively, in the X and Y directions at electron energy $E = 500$ MeV. Comparison of Figs. 3 and 4 shows that, to within experimental uncertainty, there is no change in the angular width of the PXE distribution. It follows that, at electron

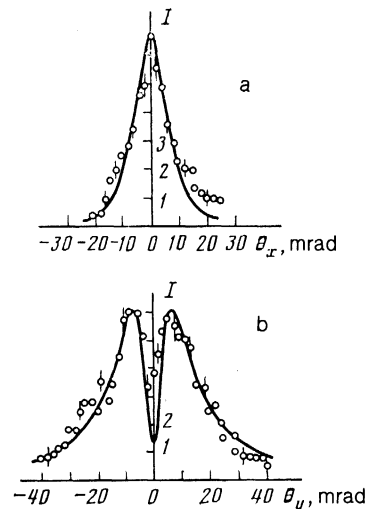


FIG. 5. Angular distribution in the (220) reflection from diamond, measured along the X direction (a), and in the (400) reflection along the Y direction (b). Solid curves—calculated angular distributions. Electron energy $E = 500$ MeV.

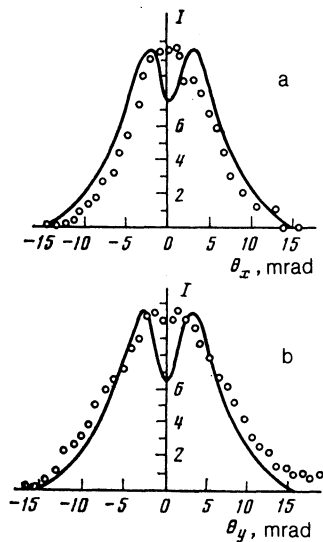


FIG. 6. Angular distribution in the (111) reflection from silicon in the horizontal (a) and vertical (b) planes. Solid curves—calculated angular distributions. Electron energy $E = 900$ MeV.

energies $E = 500$ and 900 MeV, and for diamond crystal thickness $L = 0.35$ mm, the main contribution to the angular distribution is probably due to the term on the right-hand side of (2), which is inversely proportional to the square of the PXE frequency ω_B .

Figures 6 and 7 show the angular distributions of PXE photons for the (111) and (220) reflections in silicon single crystal at $E = 900$ MeV. In contrast to diamond, the x-ray spectrometer was placed at $\theta = 90^\circ$ to the electron beam. The corresponding PXE photon frequencies were $\omega_{111} = 12$ keV and $\omega_{220} = 19.5$ keV. The angular distributions of Figs. 6a and 7a were obtained by moving the detector in the horizontal X plane, i.e., in the plane containing the momentum of the electron and the reciprocal lattice vector of the crystal. The detector collimator slit was perpendicular to this plane. The total widths at half-height of the measured angular distributions were $\Delta\theta_x = 11 \pm 0.5$ mrad for the (111) reflection and $\Delta\theta_x = 10 \pm 0.5$ mrad for the (220) reflection. Figures 6b and 7b show the corresponding vertical distributions

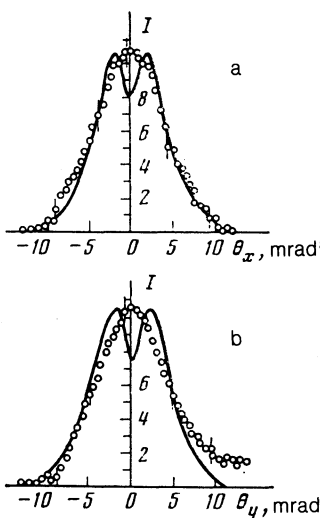


FIG. 7. Angular distribution in the (220) reflection from silicon. The notation is the same as in Fig. 6.

of the PXE yield in the Y direction. The slit collimator was horizontal in this case. The measured widths at half-height of the angular distributions were, in this case $\Delta\theta_y = 15 \pm 0.5$ mrad for the (111) reflection and $\Delta\theta_y = 10 \pm 0.5$ mrad for the (220) reflection. It is clear that, for the (220) reflection, the horizontal and vertical projections of the PXE distributions were practically identical. A certain asymmetry was found for the (111) reflection: the PXE angular distribution was found to be elongated in the Y direction, and there was an appreciable splitting into two beams, although the depth of the central valley was small. The central minimum was not seen for the (220) reflection. In this respect, the measured PXE angular distributions differ from those calculated theoretically⁶ (solid curves), which do show an appreciable valley at $\theta_{x,y} = \theta_B$ but, otherwise, the measured and calculated distributions are in good agreement. The above discrepancy may partly be due to insufficient angular resolution of the detector (2 mrad) and the greater contribution of real bremsstrahlung photons.

4. CONCLUSION

The important conclusion that may be drawn from these results is that the widths of the actual PXE angular distributions are greater by an order of magnitude than the quantity $\gamma^{-1} = m_0c^2/E$ which was considered in early theoretical papers (see the references quoted in Refs. 8–10) to be the dominant factor governing the angular divergence of PXE. Our experiments shows that the PXE angular distributions are actually determined by the influence of the second and third terms in (2), which are very similar, i.e., the PXE angular distributions are determined largely by the multiple-scattering angle $\theta_s^2 = (E_s/E)^2 (L/L_R)$ and the ratio ω_p/ω_B of the plasma frequency to the frequency of the PXE photons. In this respect, PXE differs from the usual transition radiation in a layered target⁴ whose angular width is determined by γ^{-1} , and the radiation intensity of the axis is zero. Our measured angular distributions of x-ray photons are in qualitative agreement with theoretical data. The quantitative discrepancy between the measured angular distributions and PXE theory will require further investigation.

The authors are greatly indebted to A. N. Didenko for support and discussions, and to the synchrotron staff, headed by N. A. Lashuk, for providing them with experimental facilities.

¹G. N. Kulipanov and A. N. Skrinskii, *Usp. Fiz. Nauk* **122**, 369 (1977) [*Sov. Phys. Usp.* **20**, 559 (1977)].

²V. A. Bazylev and N. K. Zhevago, *Usp. Fiz. Nauk* **137**, 605 (1982) [*Sov. Phys. Usp.* **25**, 565 (1982)].

³A. I. Akhiezer and N. F. Shul'ga, *Usp. Fiz. Nauk* **137**, 561 (1982) [*Sov. Phys. Usp.* **25**, 541 (1982)].

⁴G. M. Garibyan and Yan Shi, *Transition X-Ray Emission* [in Russian], Academy of Sciences of the Arm. SSR, Erevan, 1983.

⁵P. G. Ebert, M. G. Moran, B. A. Dahling, *et al.*, *Phys. Rev. Lett.* **54**, 893 (1985).

⁶V. L. Ginzburg and V. N. Tsytovich, *Transition Radiation and Transition Scattering* [in Russian], Nauka, Moscow, 1984.

⁷Ya. B. Faïnberg and N. I. Khizhnyak, *Zh. Eksp. Teor. Fiz.* **32**, 883 (1957) [*Sov. Phys. JETP* **5**, 720 (1957)].

⁸V. G. Baryshevsky and J. D. Feranchuk, *J. Phys. (Paris)* **44**, 913 (1983).

⁹J. D. Feranchuk and A. V. Ivashin, *Nucl. Instrum. Methods* **228**, 490 (1985).

- ¹⁰V. G. Baryshevsky and J. D. Feranchuk, *J. Phys. (Paris)* **46**, 1981 (1985).
- ¹¹S. A. Vorob'ev, B. N. Kalinin, S. D. Pak, and A. P. Polylytsyn, *Pis'ma Zh. Eksp. Teor. Fiz.* **41**, 3 (1985) [*JETP Lett.* **41**, 1 (1985)].
- ¹²Yu. N. Adishchev, V. G. Baryshevskii, S. A. Vorob'ev, *et al.*, *Pis'ma Zh. Eksp. Teor. Fiz.* **41**, 295 (1985) [*JETP Lett.* **41**, 361 (1985)].
- ¹³D. I. Adeishvili, S. V. Blazhevich, V. F. Boldyshev, *et al.*, Proc. Sixteenth All-Union Conf. on the Physics of Interaction Between Charged Particles and Single Crystals [in Russian], Moscow State University, 1986, p. 829.
- ¹⁴Yu. N. Adishchev, S. A. Vorob'ev, B. N. Kalinin, *et al.*, *Zh. Eksp. Teor. Fiz.*, **90**, 829 (1986) [*Sov. Phys. JETP* **63**, 484 (1986)].
- ¹⁵V. G. Baryshevsky, V. A. Danilov, O. L. Ermakovich, *et al.*, *Phys. Lett. A* **110**, 477 (1985).
- ¹⁶Yu. N. Adishchev, S. A. Vorob'ev, B. N. Kalinin, *et al.*, *Yad. Fiz.* **35**, 108 (1982) [*Sov. J. Nucl. Phys.* **35**, 63 (1982)].
- ¹⁷A. I. Abramov, Yu. A. Kazanskiĭ, and E. S. Matusевич, *Fundamentals of Experimental Methods in Nuclear Physics* [in Russian], Atomizdat, Moscow, 1977.
- ¹⁸P. Quittner and R. E. Wainerdi, *Atom. Energ. Rev.* **8**, 361 (1970).

Translated by S. Chomet